Colored Rubber Vulcanizates with Some Magnetic Properties

S. H. El-Sabbagh,[1] N. M. Ahmed,[1] W. M. Daoush[2]

[1]*Polymers and Pigments Department, National Research Centre, Dokki, Cairo, Egypt*
[2]*Powder Technology Department, Central Metallurgical R & D Institute (CMRDI), Cairo, Egypt*

Received 17 November 2005; revised 16 January 2006; accepted 17 January 2006
Published online 00 Month 2006 in Wiley InterScience (www.interscience.wiley.com).
DOI 10.1002/app.24207

ABSTRACT: A new composite based on natural rubber vulcanizates loaded with the newly prepared iron oxide–aluminum oxide (Fe_2O_3·Al_2O_3) fillers were prepared and their physical and magnetic studies were investigated. The prepared fillers were evaluated as reinforcing fillers with some magnetic properties; these properties were dependent on the ratio of iron oxide to aluminum oxide in each prepared ratio of these fillers. Rheological properties of rubber mixes containing ($1Fe_2O_3$:$3Al_2O_3$) and ($1Fe_2O_3$:$1Al_2O_3$) fillers exhibited better properties than mixes containing ($3Fe_2O_3$:$1Al_2O_3$) and (α-Fe_2O_3), which showed almost the same behavior. Physical properties such as tensile strength, stress at 100 and 200% strain, Young's modulus, and hardness were increased by increasing the volume fraction of the investigated fillers concentration in the mixed vulcanizates. Measured rheological and physical results were inversely related to the magnetic properties. © 2006 Wiley Periodicals, Inc. J Appl Polym Sci 102: 494–505, 2006

Key words: Fe_2O_3·Al_2O_3-rubber vulcanizates; volume fraction; filler; magnetic properties

INTRODUCTION

Fillers are commonly classified into organic and inorganic. The reinforcement of rubber by filler is associated with chemical and physical interactions between the rubber and the filler that usually rely on the physicochemical characteristics of the filler and the chemical nature of the rubber. On the other hand, incorporation of filler in elastomers results in a profound effect on mechanical and physical properties of the formed composites.[1,2]

Magnetic powders are inorganic materials that can be embedded in a polymeric matrix imparting special qualities to polymer composites. These fillers enhance properties such as thermal conductivity, electrical conductivity, response to magnetic fields, heat capacity, etc.[2] The mechanical properties of the composite are usually dependent on the polymeric phase and the magnetic effect of the inorganic filler. These magnetic powders may include ferrites and intermetallic composites of rare earths. Magnetic powders have a wide range of applications in engineering and medicine.[3,4] The colored natural iron oxides are earth pigments that are stable under all conditions practically encountered in commercial applications and have magnetic characteristics. They are unaffected chemically or physically by acids, alkalis, sunlight, or moisture, easily wetted and dispersed[5–7] with relatively low cost, while alumina is a very light element possessing no magnetic character but a unique flaky structure.[6]

However, metal-filled composites are used as antistatic materials in airplanes tires and blades to dissipate the electrostatic charges accumulated during flight.[8] Magnetic fillers are widely used in various fields to modify selected physical properties to reduce cost, and they are usually blended with polymeric materials to obtain composites. The mechanical properties of these composites depend strongly on polymer matrix properties, type of magnetic fillers, and interfacial interaction between the components. Also, the surface of the filler is the primary factor to control the mean distance between particles.[9,10]

Natural rubber (NR) is widely used in various applications particularly for tires because of its excellent elastic properties over other synthetic counterparts. However, its nonpolar character limits its application due to poor oil resistance and high permeability.[11] NR as a matrix can be mixed with fillers based on iron oxide and formulations based on these two components are considered economically feasible, as they are based on abundant natural resources.

Since ceramic magnetic materials can not be molded into complex shapes, rubber ferrite composites can replace them where shape is an important criterion.[12]

In this article, NR vulcanizates loaded with newly prepared filler based on the combination between iron oxide and aluminum oxide (Fe_2O_3·Al_2O_3) in different

Correspondence to: N. M. Ahmed (nivinahmed@yahoo.com).

ratios using solid–solid interaction process in their preparation were prepared. Colored rubber composites were studied, and their rheological, mechanical, and magnetic properties were evaluated.

EXPERIMENTAL

Materials

1. NR: Ribbed smoked sheets (RSS-1) with specific gravity 0.913, Mooney viscosity M_L (1 + 4), 60–90 at 100°C, and T_g −75°C.
2. Fillers: Iron oxide calcinated with alumina at 1000–1200°C to form a solid solution-based pigment. α- Fe_2O_3, the naturally abundant hematite form.
3. Plasticizer: Dibutylphthalate (DBP) with specific gravity 1.04 and bp 340°C.

The other rubber ingredients were customarily used in rubber industries; the solvents and chemicals were of pure grades.

Techniques

All rubber mixes were prepared on a laboratory two-roll mill of 470 mm diameter and 300 mm working distance. The speed of the slow roller was 24 rpm, with a 1:1.4 gear ratio. The rubber was mixed with ingredients according to ASTM (D15–72) and careful control of temperature, nip gap, and sequenced addition of ingredients.

Vulcanization was carried out in a single-daylight electrically heated auto controlled hydraulic press at (142 ± 1)°C and pressure 4 MPa. The compounded rubber and vulcanizates were tested according to standard methods, namely

1. [ASTM D2084–95 (1994)] for determination of rheometric characteristic using a Monsanto Rheometer model 100.
2. [ASTM D412–8a (1998)] for determination of physicomechanical properties using Zwick tensile testing machine (model-1425).
3. Hardness was determined according to [ASTM D 2240–97 (1997)].
4. Tear resistance [ASTM D 624 (1998)].
5. Permanent set [ASTM D 395 (1998)].
6. Magnetic properties (specific saturation induction B_s, retintivity B_r, relative permeability μ, and coercive force H_c) were measured for both the prepared filler materials in powder form and the related rubber-based composites (in the bulk form) by using a vibrating sample magnometer (VSM) model (LDJ 9600–1). The external field strength was 1.6 T for all measurements with 1 emu (electrical magnetic unit) magnetization range.

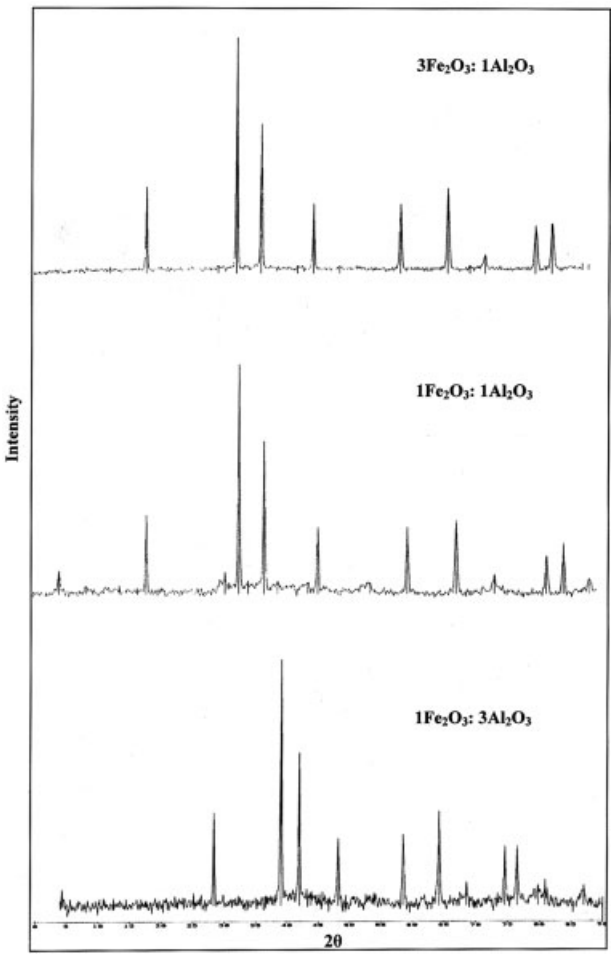

Figure 1 XRD of Fe_2O_3:Al_2O_3 pigments.

Instrumental analysis

X-ray diffraction. The powder pigment samples were tested using X-ray powder diffraction patterns at room temperature using a Philip's diffractometer (type PW1390), employing Ni-filtered Cu Kα radiation (λ = 1.5404 Å).The diffraction angle 2θ was scanned at a rate of 4° per minute.

Transmission electron microscopy. Pigments were examined using the transmission electron microscope (EM 10 Zeiss, West Germany).

Scanning electron microscopy. The samples were examined using scanning electron microscope (JEOL JX 840) and micro-analyzer electron probe.

Methods for pigment evaluation. The methods include specific gravity [ASTM D 153–54 (1981)], oil absorption [DIN EN ISO 787 (1980)], and bulking value [ASTM D 16–62 (1980)].

RESULTS AND DISCUSSION

Pigment preparation

Salts of iron and aluminum were combined together according to the selected concentrations and stoichio-

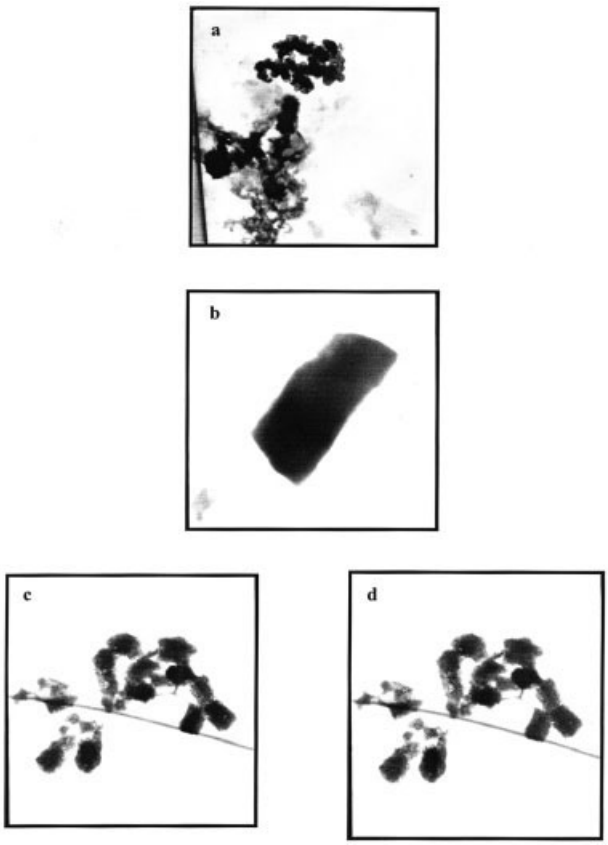

Figure 2 TEM electron micrographs of (A) Fe_2O_3, (B) $1Fe_2O_3$:$1Al_2O_3$, (C) $3Fe_2O_3$:$1Al_2O_3$, and (D) $1Fe_2O_3$:3 Al_2O_3 at magnification $\times 4 \times 10^4$.

metric ratios to prepare $Fe_2O_3 \cdot Al_2O_3$ pigments. These salts were ground together very well, and then calcined in an electric furnace for 3–5 h at 1000–1200°C. The ramp was 20°C/min.

$$2FeR \xrightarrow[O_2]{>500^\circ C} \alpha\text{-}Fe_2O_3 \xrightarrow[\text{vacuum}]{>1000^\circ C} Fe_3O_4(\text{magnetite})$$

$$2Al(OH)_3 \xrightarrow{>500^\circ C} \gamma\text{-}Al_2O_3 + 3H_2O$$

$$\gamma\text{-}Al_2O_3 \xrightarrow{1200^\circ C} \alpha\text{-}Al_2O_3$$

In case of mixing the two compounds, the solid–solid interaction took place according to the following equation:

$$x\ Fe_2O_3 + (1-x)Al_2O_3 \xrightarrow{1000^\circ C} [(Al)_{1-x}(Fe)_x]_2O_3$$

where R = CH_3COO^-, NO_3^-, SO_4^{2-}, OH^-,. . . etc.

Both oxides have trigonal structure, which led to an easy interference between them, so that one of them can replace the other in its crystal structure according to the selected concentration for each compound, through a solid–solid solution interaction, giving a solid more stable than any of its components.

X-ray diffraction of different samples of iron-aluminum oxide pigments

The "*d*" values and relative intensities I/I_o of X-ray pattern for samples of prepared pigments were illustrated in Figure 1, and the data showed that for the three mixtures including $3Al_2O_3$:$1Fe_2O_3$, $1Al_2O_3$:$1Fe_2O_3$, and $1Al_2O_3$:$3Fe_2O_3$, the calcinations of these mixtures resulted in one solid solution in each case without the appearance of any crystalline phase beside it. This indicated that the mixing of any proportion of the components easily forms this solid solution. The *d*-values of the formed solid solutions were located between the *d*-values of α-Al_2O_3 and α-Fe_2O_3, as indicated from ASTM patterns.

Electron microscopy

Electron microscope technique was used in this work to identify the morphology of the particles of the concerned pigments. Figures 2(a)–2(d) showed the particle shapes of prepared iron-aluminum oxide pigments, viewed through a TEM at a magnification 5 $\times$ 10^4. As seen, from the figures, the shape of the prepared pigments was platy. This platy structure provided a reinforcing effect and seemed as fibers

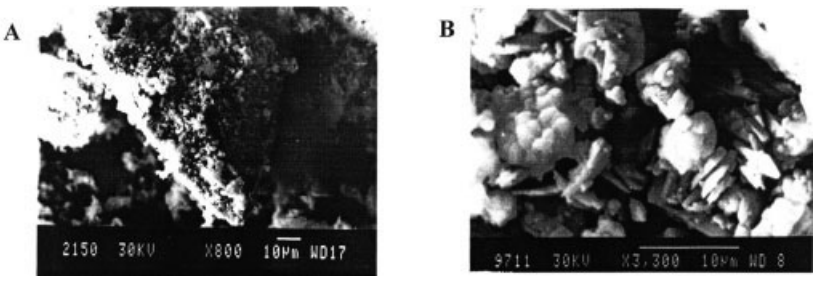

Figure 3 Scanning electron micrographs of $1Fe_2O_3$:$1Al_2O_3$ pigment at magnifications (A) $\times$800 and (B) $\times$3300.

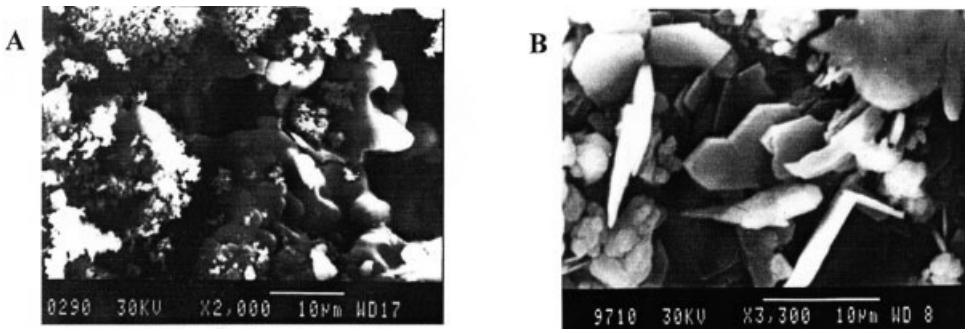

Figure 4 Scanning electron micrographs of $3Fe_2O_3$:$1Al_2O_3$ pigment at magnifications (A) ×2000 and (B) ×3300.

linking the matrix tightly. These particles were so fine that they appeared in aggregations as appeared in three-dimensional SEM micrographs showed in Figures 3–5, which were in agreement with the previous figures confirming the platy structure of the prepared pigments. The fineness of the prepared fillers allowed them to give more homogenous texture to the rubber composite, rendering it with better mechanical properties.

Evaluation of iron-aluminum oxide fillers

Prepared fillers were evaluated in comparison with red iron oxide and aluminum oxide according to standard methods. The characteristics of the evaluated pigments are summarized in Table I.

From Table I, it is clear that

1. The prepared fillers showed higher values of oil absorption, lower specific gravity values, and higher bulking values than that of red iron oxide, but lower oil absorption and moderate specific gravity than that of aluminum oxide.
2. Oil absorption showed the highest value for the fillers containing Al_2O_3, followed by $1Fe_2O_3$:$3Al_2O_3$, because as the alumina percentage in the pigment increases, oil absorption also increases, this may be due to that alumina particles are so fine and light, i.e., need more oil.
3. Specific gravity values were high, since iron is a heavy element, but as the percentage of alumina increased in the compound, specific gravity showed lower values, rendering filler particles dispersed more homogenously in the surrounding media leading to more fine texture or matrix.

Rheological properties of NR loaded with investigated fillers

Raw rubber had poor rheological and mechanical properties; filler must be added to improve these properties, since it had an important direct action on these properties.

In this work, the prepared fillers were added in relatively large proportions to act as a reinforcing agent in rubber composites. A detailed study was carried out to highlight the effect of these prepared fillers on the physical and rheological properties of NR vulcanizates. Table II summarized the mixed formulations as well as their rheometric characteristics at (142 ± 1)°C. The data revealed that an increase in filler content led to an increase in the maximum, minimum torque, and optimum cure time, i.e., the increase of iron content led to an increase in these properties. The rate of vulcanization change was dependent on the ratio and type of filler used. The M_L value signifies the extent of filler–filler interaggregations[13]; therefore, the high values of M_L in case of $1Fe_2O_3$:$3Al_2O_3$ is due to

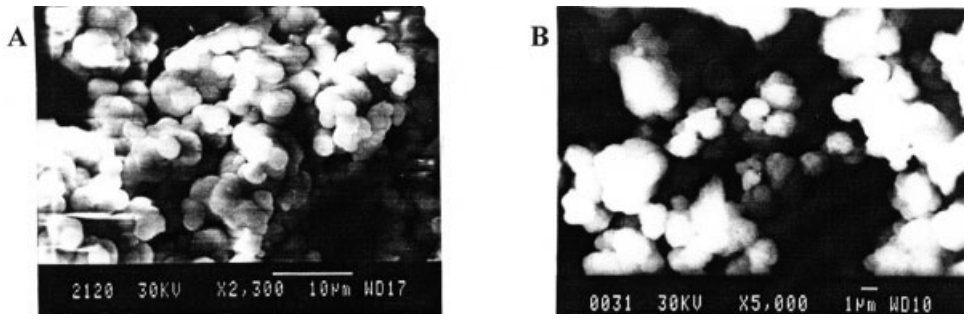

Figure 5 Scanning electron micrographs of $3Fe_2O_3$:$3Al_2O_3$ pigment at magnifications (A) ×2300 and (B) ×5000.

TABLE I
Characteristics of Prepared Fe_2O_3:Al_2O_3 Pigments

Materials	Oil absorption (g/100g)	Specific Gravity	BV (gal/100 b)	pH
Fe_2O_3	16	4.35	2.7701	11
Al_2O_3	54.52	3.12	3.8672	11
$1Fe_2O_3$:$1Al_2O_3$	20	3.82	3.1544	11
$3Fe_2O_3$:$1Al_2O_3$	18	4.65	2.9731	11
$1Fe_2O_3$: $3Al_2O_3$	32	4.00	4.0436	11

high degree of filler–filler interaggregations. Vulcanizates containing $1Fe_2O_3$:$1Al_2O_3$ have M_L values slightly lower than those of $1Fe_2O_3$:$3Al_2O_3$, thereby indicating reduction in the filler–filler interaggregations.[13]

In other words, minimum torque determined from a Monsanto Oscillating-Disc-Rheometer was a measure of the compound viscosity. Relative minimum torque D^R_{min} can be calculated as a function of filler loading, which is shown in Figure 6 and expressed in eq. (1).

$$D^R_{min} = \left(\frac{D^F_{min}}{D^o_{min}}\right) - 1 \quad (1)$$

where D^F_{min} is the minimum torque of the filled compound and $D^\circ_{min.}$ is the minimum torque of the gum. It was observed that the relative torque increased with filler loading. Also, it increases as the ratio of alumina in the prepared pigments increases, i.e., it is the highest for vulcanizates containing $1Fe_2O_3$:$3Al_2O_3$, and the lowest for vulcanizates containing Fe_2O_3.

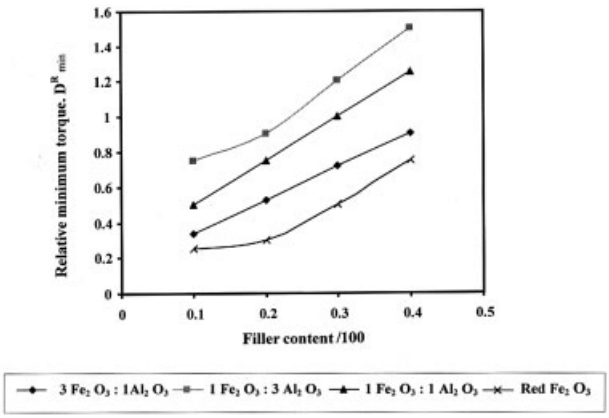

Figure 6 Relative minimum torque of curometer measurements as a function of Fe_2O_3:Al_2O_3 filler loading.

Incorporation of prepared fillers into rubber composite led to an increase in curometer torque during vulcanization. The ratio between the torque of the loaded compound and that of gum was found to be directly proportional to filler loading. The slope of the linear plot shows an increase in the relative torque as a function of the filler loading. This relation was defined by Wolff[13] as

$$D = \frac{D_{max} - D_{min}}{D^o_{max} - D^o_{min}} - 1 = \alpha_F \frac{m_F}{m_P} \quad (2)$$

where $(D_{max} - D_{min})$ is torque difference of the filled, $(D^\circ_{max} - D^\circ_{min})$ is torque difference of the gum; m_F/m_P is filler loading. α_F is a filler specific constant that is

TABLE II
Formulations and Rheological Characteristics of Natural Rubber (NR) Vulcanizates

	Ingredient (phr)				Rheometric characteristics (142 ± 1°C)				
	$3Fe_2O_3$:$1Al_2O_3$	$1Fe_2O_3$:$3Al_2O_3$	$1Fe_2O_3$:$1Al_2O_3$	redFe_2O_3	M_L (dN m)	M_H (dN m)	T_{s2} (min)	T_{c90} (min)	CRI (min^{-1})
F0	–	–			1	41	2	4.75	36.4
F1	10	–			1.25	48.85	2.687	5	34.23
F2	20	–			1.52	51.25	2.625	5.5	34.78
F3	30	–			1.6	53.3	2.56	5.75	31.37
F4	40	–			1.925	55.725	2.54	5.87	29.96
F5	–	10			1.75	50.57	2.5	5.5	33.33
F6	–	20			1.9	54.55	2.43	5.375	33.89
F7	–	30			2.2	58	2.313	5.25	34.04
F8	–	40			2.5	61.25	2.25	5	36.36
F9			10	–	1.5	50.25	2.73	5.875	31.49
F10			20	–	1.75	53.5	2.69	5.75	32.65
F11			30	–	2	56	2.56	5.5	34.04
F12			40	–	2.25	59	2	4.5	40
F13			–	10	1.25	48.1	2.5	5.375	34.78
F14			–	20	1.3	49.9	2.438	5.5	32.65
F15			–	30	1.5	52	2.375	5.75	29.36
F16			–	40	1.75	53	2.313	5.875	28.07

Base recipe in phr: NR, 100; stearic acid, 1; zinc oxide, 5; (*N*-cyclohexyl 2-benzothiazole sulfonamide) CBS, 0.8; sulfur, 1.5; oil, 3. M_L, minimum torque; M_H, maximum torque; t_{s2}, scorch time; t_{c90}, optimum cure time; and CRI, cure rate index.

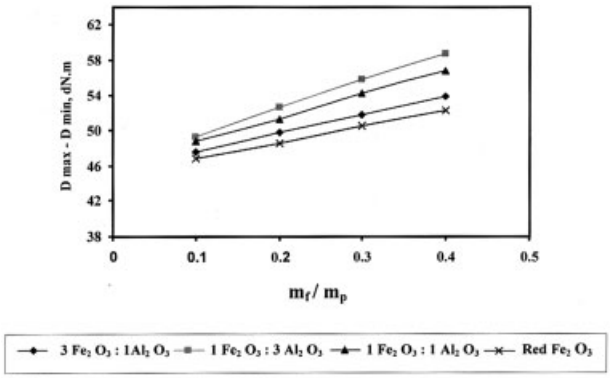

Figure 7 Maximum change in curometer torque during vulcanization as a function of m_f/m_p for $1Fe_2O_3$:$1Al_2O_3$ loading.

independent on the cure system and closely related to the morphology of filler. The benefit of eq. (2) therefore lies not only on the fact that it defined a filler specific constant that is determined by the filler structure but also in its prediction that the degree of crosslinking density of the filler.[14] Figure 7 showed the linear relationship between ($D_{max}-D_{min}$) and investigated filler loading. Equation (2) furthermore showed that—based on a simple test—α_F can be calculated from the change in torque that occurred during vulcanization of the two compounds, both the gum and the loaded ones. The values of α_F were plotted for the investigated fillers versus volume fraction for these fillers, as shown in Figure 8, yielding four curves having completely the same patterns. From the figure, it can be indicated that α_F is higher for $1Fe_2O_3$:$3Al_2O_3$ fillers, and as the ratio of iron decreases the vulcanizates exhibit better rheological properties.

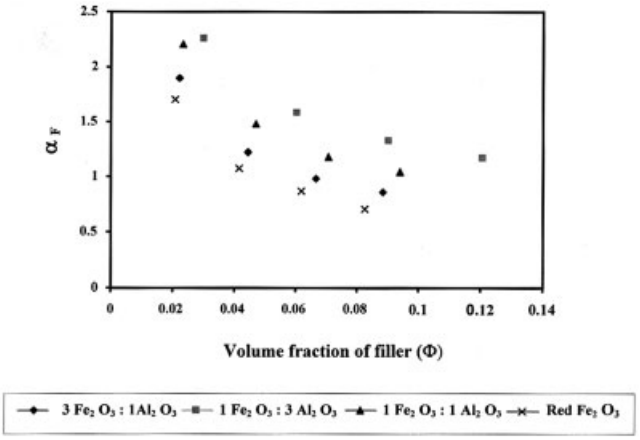

Figure 8 α_F as a function of volume fraction for $1Fe_2O_3$:$1Al_2O_3$ filler.

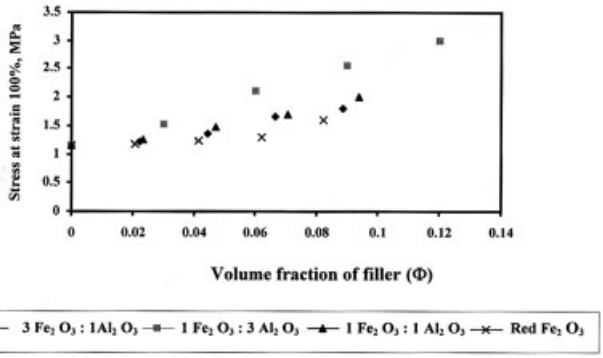

Figure 9 Stress at 100% strain as a function of volume fraction for $1Fe_2O_3$:$1Al_2O_3$ filler.

Effect of the investigated fillers on the physicomechanical properties of the NR vulcanizates

It has been accepted that the laws governing the change in elastic modulus are determined by the compounding, processing, and vulcanization conditions. Concerning the filler, the modulus of the vulcanizate should furthermore reflect the effect of filler morphology and surface activity that determines filler–polymer and aggregate–aggregate interaction.[14]

The tensile moduli at 100 and 200% strain (σ_{100} and σ_{200}), respectively, were presented in Figures 9 and 10. Since these vulcanizates were cured with the same curing system, i.e., their crosslink densities are virtually identical; the change in modulus and the strain values could only be explained by filler characteristics.

At relatively small elongations (100%), the modulus of $1Fe_2O_3$:$3Al_2O_3$ filled rubber was much higher and increased more rapidly with the increase in filler loading than for the other prepared fillers.

On the other hand, the stress at 200% strain for rubber vulcanizates loaded with $3Fe_2O_3$:$1Al_2O_3$ exhibit higher modulus, suggesting a different mechanism of the filler effect on modulus. At these elongations (200%), the effect of the interaggregate associa-

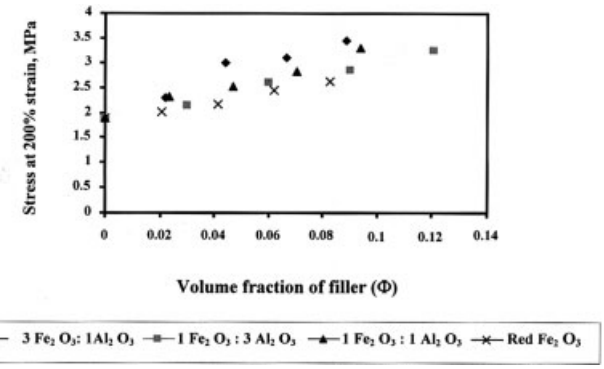

Figure 10 Stress at 100% strain as a function of volume fraction for $1Fe_2O_3$:$1Al_2O_3$ filler.

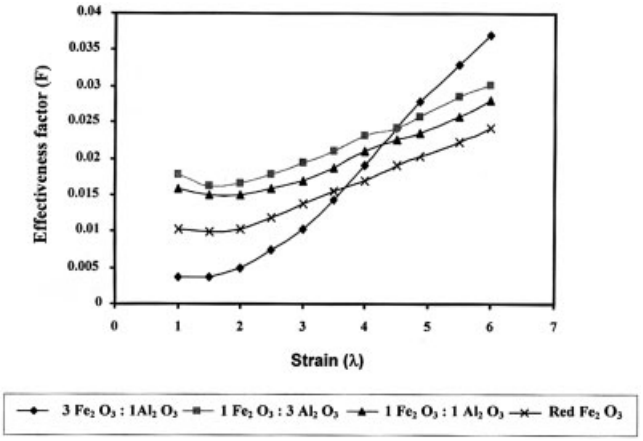

Figure 11 Effectiveness factor F for modulus as a function of strain for Fe_2O_3:Al_2O_3-filled vulcanizates.

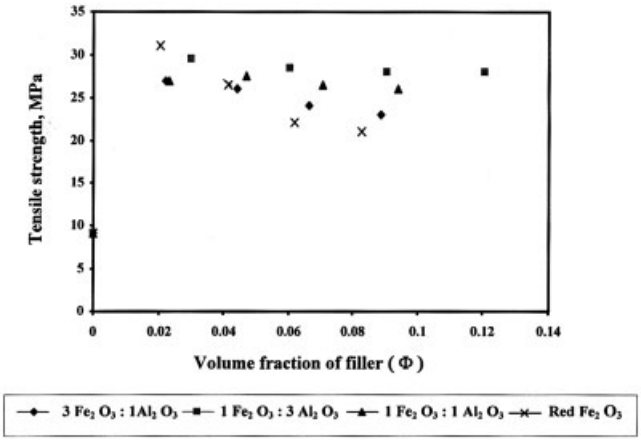

Figure 12 Tensile strength values as a function of volume fraction for $1Fe_2O_3$:$1Al_2O_3$ filler.

tion should disappear, and the interaction between polymer and filler may now play an important role in modulus. In case of rubber vulcanizates loaded with $1Fe_2O_3$:$3Al_2O_3$, the poor interaction with rubber led to slippage and deattachment of rubber molecules on the filler surface, resulting in low modulus.

Then it was obvious that the higher moduli of vulcanizates filled with $3Fe_2O_3$:$1Al_2O_3$ were certainly related to the high localized bonding between polymer and filler, caused either by strong physical adsorption or by chemisorption.[2]

It was found that the Einstein-Guth-Gold equation could be applied to the filled vulcanizates over a wide range of strains if the effective volume of the filler was introduced.[15]

$$\sigma_f = \sigma_o(1 + 2.5f\phi + 14.1f^2\phi^2) \quad (3)$$

with

$$\phi_{\text{eff}} = f\phi$$

where σ_f is the modulus of the filled vulcanizate, σ_o is the modulus of the gum, Φ is the volume fraction of the filler, Φ_{eff} is the effective volume fraction of filler, and f is the effectiveness factor for transforming Φ into Φ_{eff}.

It can be observed from Figure 11 the relation between the effectiveness factors as a function of strain. In the low strain region, the effectiveness factor increases with increasing strain, probably due to the cohesion of the filler network, while at high strain region, where crystallization and nonaffine deformation (non-Gaussian behavior) of the polymer chains were involved stress increases, which is equivalent to an apparent rise in filler volume. This effect would be diminished by deattachment and slippage of the rubber molecules on the filler surface, related to poor filler–polymer interaction.[15]

The relation between tensile strength with volume fraction of investigated filler loading was illustrated in Figure 12. The better tensile strength was achieved by NR composites filled with $1Fe_2O_3$:$3Al_2O_3$, this is due to the uniform and efficient stress transfer through a strong interfacial bond between the filler and the polymer,[2] while at 10 phr of filler loading, the maximum tensile strength was shown by composites filled with α-Fe_2O_3. Therefore, tensile strength decreases with the increase of filler loading for all investigated fillers. At higher filler loading, filler–filler interaction was responsible for the development of cracks and ultimately tended to decrease the tensile strength.[2]

The dependence of rupture strain (elongation at break) on increasing volume fraction of investigated fillers was shown in Figure 13. Generally, addition of fillers do not increase rupture strain of the rubber composite[2]; however, an opposite trend was expected in some cases. It was also found that, in all studied filled rubber systems, the rupture strain increases at first and then decreases subsequently with increasing

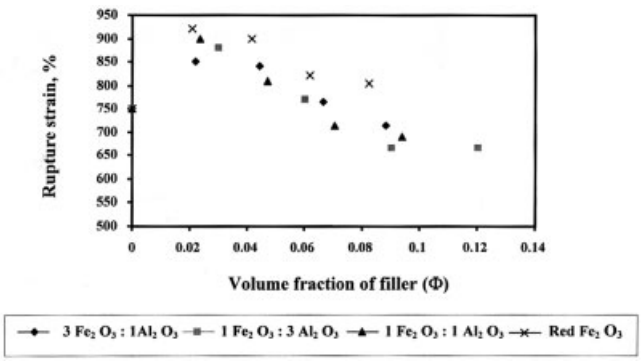

Figure 13 Rupture strain values (%) as a function of volume fraction for $1Fe_2O_3$:$1Al_2O_3$ filler.

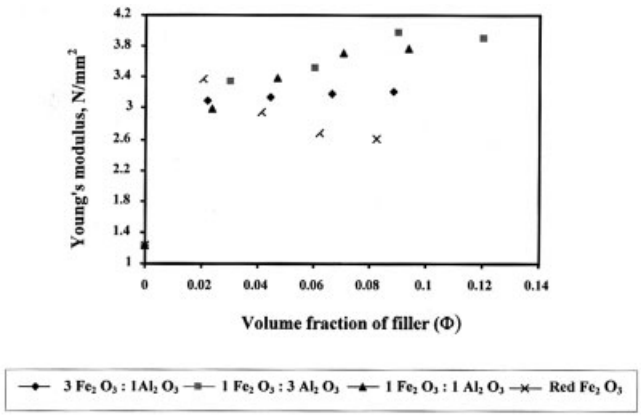

Figure 14 Young's modulus values as a function of volume fraction for Fe_2O_3·Al_2O_3 filler.

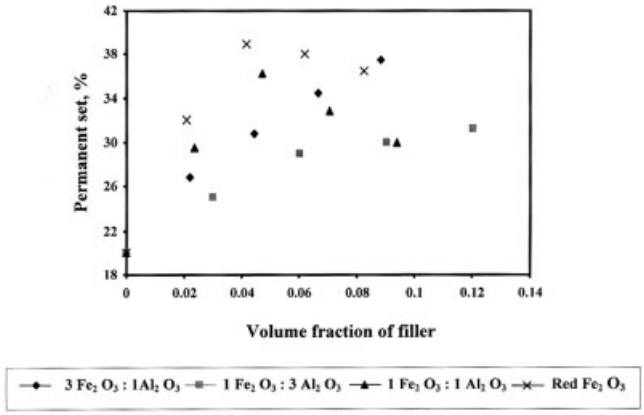

Figure 16 Variation of permanent set as a function of volume fraction for filler loading.

filler content. This is due to that filler particles prevent catastrophic failure of the specimen by arresting crack growth and increase the extendibility of the composites.[13]

The variation of Young's modulus for NR composites containing several investigated fillers with volume fraction for these filler were represented in Figure 14. The plots showed that Young's modulus increases with filler loading for $1Fe_2O_3$:$3Al_2O_3$, $1Fe_2O_3$:$1Al_2O_3$, and $3Fe_2O_3$:$1Al_2O_3$, while for red α-Fe_2O_3 Young's modulus firstly increases at 10 phr loading then decreases with further increase in volume fraction of filler.

The results of hardness versus volume fraction of filler for all filled rubber vulcanizates with Fe_2O_3·Al_2O_3 are graphically represented in Figure 15. It can be observed that, an increase in the volume fraction of prepared loaded filler increases the hardness of the composite; a similar trend was reported by Nielsen[16] in case of the rigid filler. The figure showed that, after 10 phr of filler loading, the increment in the hardness of composites filled with $1Fe_2O_3$:$3Al_2O_3$ was found to be more than that of other investigated fillers.

The permanent set that reflected the residual deformation due to the plastic part of a vulcanizate under tensile stress were demonstrated in Figure 16.

Generally, the usual measurement of set was intended to evaluate delayed elastic recovery. It was observed that the permanent set increases as volume fraction increases for $3Fe_2O_3$:$1Al_2O_3$ and $1Fe_2O_3$:$3Al_2O_3$ loaded rubber. After 20 phr of filler loading, a decrease for rubber loaded with α-Fe_2O_3 and $1Fe_2O_3$:$1Al_2O_3$ was observed. In general, for all loaded rubber vulcanizates with prepared fillers, a complete removal of the stress do not recover their initial length, i.e., a permanent set remained in it, which was originally related to flow processes (Relaxation processes).[17]

Figure 17 represented the effect of investigated fillers on tear strength. A significant increase by using these fillers was observed, which were consistent with the previous obtained results. This meant that physical properties were improved by using the investigated fillers. These results were in agreement with the rheological characteristics.

The interaction between rubber and filler has been investigated by a number of workers using a swelling

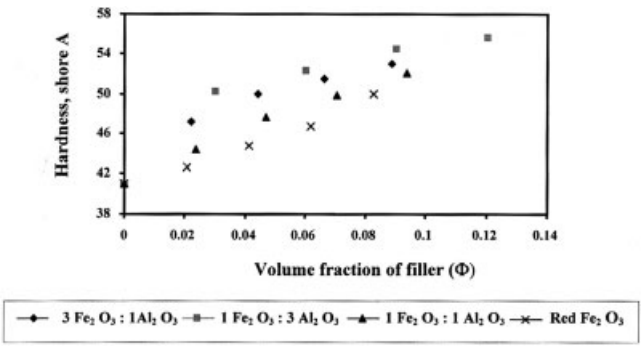

Figure 15 Shore A hardness as a function of volume fraction for filler loading.

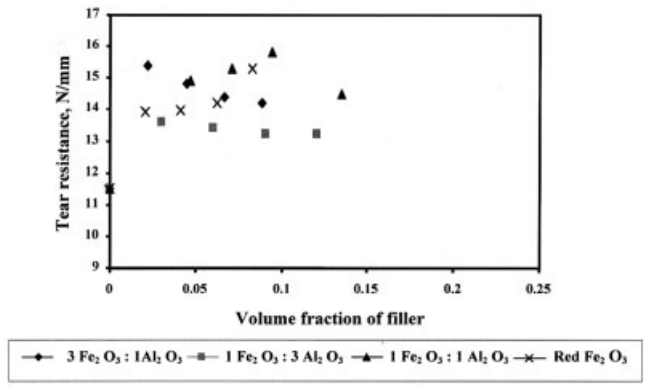

Figure 17 Tear resistance as a function of volume fraction for Fe_2O_3·Al_2O_3 filler.

TABLE III
Swelling Characteristics for (NR) Vulcanizates with and without Fillers

Sample name	No. of sample	Q_F/Q_g	$1/Q$	Soluble fraction (%)	M. wt. between crosslinking M_c (g/mole)	$v \times 10^4$ (crosslinking density; mole/cc)
Control	0	–	0.3167	4.14	4359	1.15
$3Fe_2O_3$:$1Al_2O_3$	10	0.8475	0.3612	3.12	3228	1.55
	20	0.7643	0.4005	3.16	2675	1.87
	30	0.6799	0.4503	3.10	2167	2.31
	40	0.6088	0.5028	3.05	1777	2.81
$1Fe_2O_3$:$3Al_2O_3$	10	0.7692	0.3979	3.09	2706	1.85
	20	0.7131	0.4305	3.01	2355	2.12
	30	0.6662	0.4595	2.98	2089	2.39
	40	0.6288	0.4868	2.92	1883	2.66
$1Fe_2O_3$:$1Al_2O_3$	10	0.8847	0.3459	3.96	3489	1.43
	20	0.7428	0.4124	3.88	2541	1.97
	30	0.7009	0.4367	3.81	2288	2.19
	40	0.62212	0.4920	3.77	1848	2.71
Red Fe_2O_3	10	0.8717	0.35115	4.03	3399	1.47
	20	0.7944	0.3853	3.96	2869	1.74
	30	0.72803	0.4205	3.89	2449	2.04
	40	0.6699	0.4569	3.51	2110	2.37

technique, assuming the swelling to be completely restricted at the rubber–filler interface due to adhesion. This was in accordance with the equation of Lorentz and Parks[18] studying rubber–filler interaction.

$$\frac{Q_F}{Q_g} = ae^{-z} + b$$

where Q is defined as grams of solvent per gram of rubber hydrocarbon and is calculated by [Q = (swollen weight − dried weight)/(original weight × 100/Formula weight)]. F and g refer to filled and gum mixes. Z is the weight fraction of filler in the vulcanizate, a and b are constants characteristic for the system. The effect of interaction between polymers that is incorporated with filler can be studied by the value $1/Q$.[19] The higher the Q_F/Q_g values, the lower would be the extent of interaction between filler and matrix. The values of Q_F/Q_g and $1/Q$ were calculated using the above equation and the obtained data were listed in Table III. From these data, it could be seen that, Q_F/Q_g decreases with the increase of filler loading, suggesting a swelling restriction of the rubber matrix due to the presence of the filler.

It was then observed that, the lowest value of Q_F/Q_g and the greatest one for $1/Q$ were obtained for vulcanizates containing $3Fe_2O_3$:$1Al_2O_3$, i.e., since the higher the Q_F/Q_g values, the lower would be the extent interaction between the filler and the matrix.[20]

To confirm these results, the formation of such crosslinks was determined from the equilibrium swelling measurements through the molecular weight between crosslinks, M_c, according to the Flory-Rehner relation:[20,21]

$$\frac{1}{M_c} = \frac{-1}{2\rho V_o} \frac{\ln(1 - V_R) + V_R + \mu V_R^2}{V_R^{1/3} - 1/2V_R} \quad (4)$$

The degree of crosslinking[21] is given by $\nu = \frac{1}{2M_c}$, where ρ is the density of rubber; V_o is the molar volume of swelling solvent absorbed (toluene V_o = 106.3 cm^3/mol) V_R is the volume fraction of the rubber in the swollen material, and μ is the interaction parameter constant.

The obtained data for ν were listed in Table III, where one can notice that ν increases by increasing filler content. The increase of crosslinking density in the presence of different type of fillers was due to the additional physical and chemical crosslinks as were clearly seen from swelling and M_c data given in Table III.

Magnetic properties of prepared composites

Table IV summarized the values of specific saturation induction B_s and retentivity B_r in emu/g and the coercive force H_c in Orested for the prepared fillers and the corresponding composites.

From these values, it can be observed that all the materials exhibited parasitic ferromagnetic characteristics that show antiferromagnetic ordering for the domains. Figures 18 and 19 showed the hystersis loops of prepared fillers and the corresponded rubber filled composites, respectively. The shapes shown in these figures are characteristic for antiferromagnetic particulates with canted domains ordering.[22] A field of 1.6 T cannot saturate the magnetization curves, and

TABLE IV
Magnetic Properties of the Prepared Fillers and the Corresponding Rubber-Based Composites

Materials	B_s (emu/g)	B_r (emu/g)	H_c (Oe)
α-Fe_2O_3	0.96	0.16	246
$1Fe_2O_3$:$1Al_2O_3$	0.40	0.1	3169
$3Fe_2O_3$:$1Al_2O_3$	0.44	0.13	1845
$1Fe_2O_3$:$3Al_2O_3$	0.35	0.13	3037
α-Fe_2O_3–rubber	0.46	0.027	109
$1Fe_2O_3$:$1Al_2O_3$–rubber	0.30	0.02	99
$3Fe_2O_3$:$1Al_2O_3$–rubber	0.37	0.01	61
$1Fe_2O_3$:$3Al_2O_3$–rubber	0.29	0.02	123

the magnetization still has a tendency to increase, which is characteristic of the mainly antiferromagnetic ordering of the spins in filler powders.

It was obvious that by adding the fillers to the rubber vulcanizates, properties of rubber were converted from diamagnetic in pure rubber without addition of magnetic fillers to weak ferromagnetic with different specific saturation induction properties (B_s, B_r, and H_c) depending on the concentration of the filler loaded within rubber vulcanizates, which was 40% by weight in the tested rubber samples.

Saturation magnetizations and the remanants values were higher for fillers and lower for the corresponded rubber composites, which were due to the presence of the filler powder in the rubber matrix. These values were dependent on the ratio of fillers included in the rubber composites.[23] The specific saturation induction (B_s) was greater in case of rubber composites containing higher ratios of α-Fe_2O_3 powder than those containing greater ratio of Al_2O_3. This may be due to that the relative permeability that was measured at 200 Oe of α-Fe_2O_3 powder has higher magnetic properties (3.72) exceeding that of alumina (1.17) by three times. The values of coercive force (H_c) and the retentivity (B_r) listed in Table IV showed that the coercive forces and retentivity of the composites have lower values in case of rubber composites than in the powder filler due to the increase in magnetic interaction between the filler particles with each other than interaction between filler and rubber in the formed rubber composites. It was then obvious that, rubber vulcanizates filled with $3Fe_2O_3$:$1Al_2O_3$ showed better magnetic properties than those loaded with $1Fe_2O_3$:$1Al_2O_3$ and both are better than those loaded with Fe_2O_3:$3Al_2O_3$.

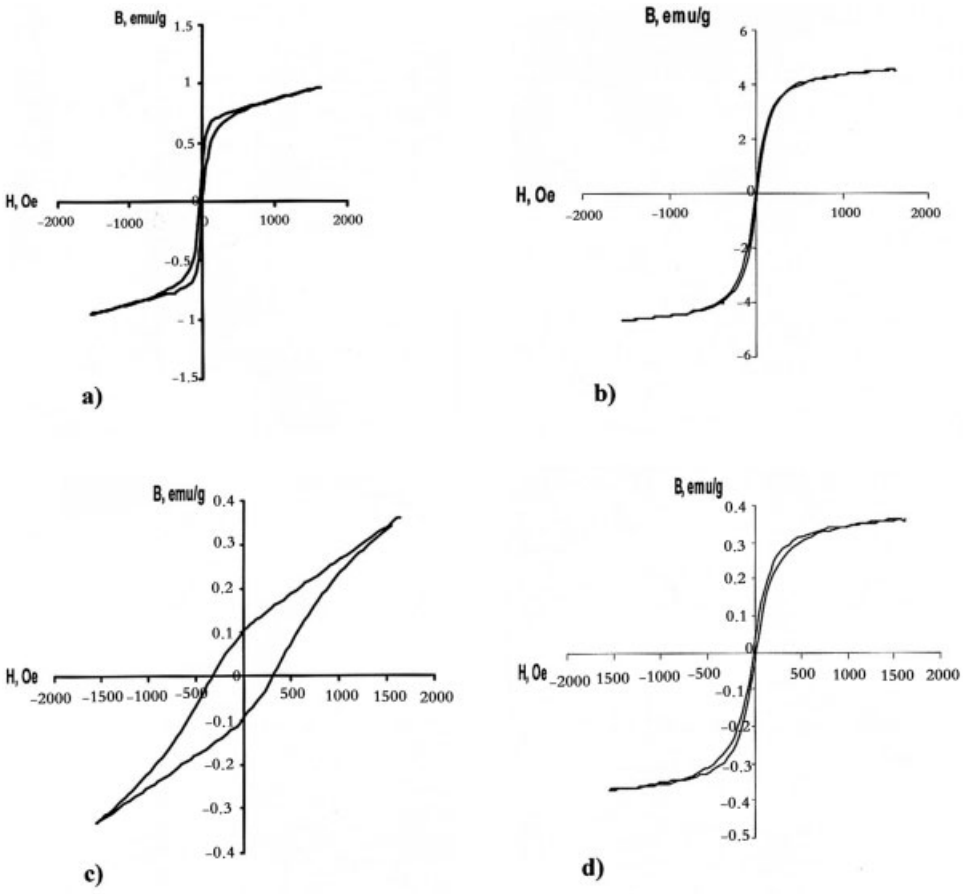

Figure 18 The magnetic hystersis loopes for (a) α-Fe_2O_3, (b) $1Fe_2O_3$:$1Al_2O_3$, (c) $3Fe_2O_3$:$1Al_2O_3$, and (d) $1Fe_2O_3$:$3Al_2O_3$, respectively.

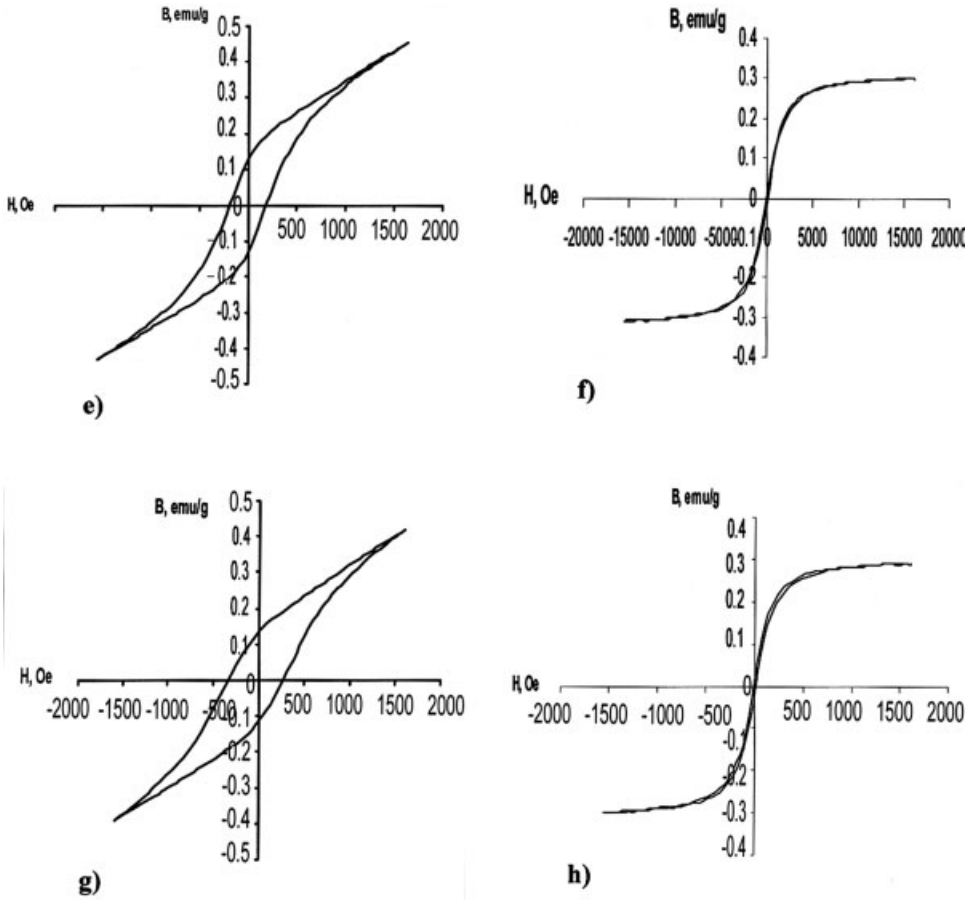

Figure 19 The magnetic hystersis loopes for rubber vulcanizates loaded with 40% (a) α-Fe_2O_3, (b) $1Fe_2O_3$:$1Al_2O_3$, (c) $3Fe_2O_3$:$1Al_2O_3$, and (d) $1Fe_2O_3$:$3Al_2O_3$, respectively.

CONCLUSIONS

From this article, it can be concluded that

1. The incorporation of Fe_2O_3·Al_2O_3 solid solution fillers onto NR vulcanizates improved their rheological properties.
2. The value of α_F (rubber-filler interaction) showed that the best Fe_2O_3:Al_2O_3 fillers loaded in rubber vulcanizates can be ordered as follows: vulcanizates containing $1Fe_2O_3$:$3Al_2O_3$, $1Fe_2O_3$:$1Al_2O_3$, $3Fe_2O_3$:$1Al_2O_3$ and then vulcanizates containing α-Fe_2O_3. This behavior was the opposite on measuring the magnetic properties, i.e., each prepared ratio of fillers gave rubber vulcanizates a characteristic property.
3. The tensile studies indicated that the serviceability of the elastomer was affected in vulcanizates loaded with filler from 10 to 40 phr. Changing in the tensile strength, rupture strain, and Young's modulus of the rubber- Fe_2O_3·Al_2O_3 composites with the volume fraction of prepared fillers was high in rubber composites filled with α-Fe_2O_3 and $1Fe_2O_3$:$3Al_2O_3$. The initial increase in these properties were due to the increase in the stress-induced crystallization of the NR matrix and it was supported by the change in molecular weight. The value of tensile strength or rupture strain was decreased with the increase of filler loading.
4. NR vulcanizates loaded with Fe_2O_3:Al_2O_3 fillers showed an increase in crosslinking (by swelling measurements), indicating an interaction or bonding between the rubber and fillers.
5. The stiffening of rubber, permanent set, and tear strength changed according to the type of prepared fillers (the ratio of iron oxide to that of alumina).
6. Addition of filler powder converted the nonmagnetic rubber composites to magnetic ones with ferromagnetic properties.
7. Rubber–Fe_2O_3:Al_2O_3 vulcanizate's ferromagnetic properties can be arranged as follows. Rubber–$3Fe_2O_3$:$1Al_2O_3$ > Rubber–$1Fe_2O_3$:$1Al_2O_3$ > Rubber–$1Fe_2O_3$:$3Al_2O_3$.

The authors wish to express their deep thanks to Prof. Dr. A.F. Younan, Polymer and Pigment Department, National

Research Center, and Prof. Dr. S.F. Moustafa, Powder Technology department, Central Metallurgical R & D Institute (CMRDI), for their kind help in revising this article.

References

1. Sombatsompop, N.; Thongsang, S.; Markpin, T.; Wimolomala, E. J Appl Polym Sci 2004, 93, 2119.
2. Hundiwale, D. G.; Kapadi, U. R.; Desai, M. C.; Patil, A. G.; Bidkar, S. H. Polym Plast Technol Eng 2004, 43, 615.
3. Betancourt-Galinde, R.; Saldivar, R.; Rodriguez-Fernàndez, O. S.; Ramos-de vallè, L. F. Polym Bull 2004, 51, 395.
4. Naik, R.; Kroll, E.; Rodak, D.; Tsoi, G. M.; McCullen, E.; Suryanarayanan, R. J Magn Magn Mater 2004, 272–276, 1239.
5. Rammelt, U.; Reinhardt, G. Prog Org Coat 1994, 24, 309.
6. Morgan, W. M. In Outlines of Paint Technology, 3rd ed.; Edward Arnold, a division of Hodder & Stoughtan: London, 1990; Chapter 2, p 158.
7. Patton, T. C. Pigment Handbook; Wiley Interscience: New York, 1973; Vol. 3, 2, p 861.
8. Vinod, V. S.; Varghese, S.; Kuriakose, B. J Appl Polym Sci 2004, 91, 3156.
9. Cao, X.; Luo, Y.; Feng, L. J Appl Polym Sci 1999, 74, 3412.
10. Makled, M. H.; Matsui, T.; Tsuda, H.; Mabuchi, H.; El-Mansy, M. K.; Morii, K. J Mater Process Technol 2004, 5, 1.
11. Sindnu, S.; Anantharaman, M. R.; Thampi, B. P.; Malini, K. A.; Kurian, P. Bull Mater Sci 2002, 25, 599.
12. Mohammed, E. M.; Malini, K. A.; Kurian, P.; Anantharaman, M. R. Mater Res Bull 2002, 37, 753.
13. Wolff, S.; Wang, M. J. Rubber Chem Technol 1992, 65, 329.
14. Wolff, S. Rubber Chem Technol 1996, 69, 325.
15. Bandyopadhyay, S.; De, P. P.; Tripathy, D. K.; De, S. K. Rubber Chem Technol 1996, 69, 637.
16. Nielsen, L. E.; Landel, R. F. In Mechanical Properties of Polymers and Composites, 2nd ed.; Marcel Dekker: New York, 1994; p 437.
17. Tager, A. Physical Chemistry of Polymers; Mir publishers: Moscow, 1978; p 204.
18. Lorentz, O.; Parks, C. R. J Polym Sci 1961, 50, 299.
19. Parks, C. R. J Rubber Chem Technol 1982, 55, 1170.
20. Ismail, H.; Jaffri, R. M.; Rozman, H. D. J Elastomer Plast 2003, 35, 181.
21. Zhag, G. A.; Zhou Zhou, M. H.; Ma, J. H.; Liang, B. R. J Appl Polym Sci 2003, 90, 2241.
22. Deng, Y.; Wang, L.; Yang, W.; Fu, S.; Elaïssari, A. J Magn Magn Mater 2003, 257, 69.
23. Mary, M. In Scientific and Clinical Applications of Magnetic Carriers; Hafeli, U., Schutt, W., Zborowski, M., Eds.; Plenum: New York, 1997; p 303.